ELSEVIER

Thermochimica Acta 334 (1999) 49–55

thermochimica acta

www.elsevier.com/locate/tca

Heat diffusion analysis of the temperature distribution and phase lag build-up in TMDSC specimens

Frédéric U. Buehler, James C. Seferis*

Department of Chemical Engineering, Polymeric Composites Laboratory, University of Washington, Box 351750, Seattle, WA 98195-1750 USA

Received 15 September 1998; accepted 16 April 1999

Abstract

In the present study, a complete model of thermal diffusion in a TMDSC specimen was developed. The numeric simulation of the temperature evolution takes into account the transient terms at early times and assesses the time at which these vanish. The simulation also provides a complete temperature profile in both radial and axial direction within a cylindrical specimen, and underlines the existence of non-negligible temperature gradients within a polymeric sample. The model predicts a heat flow phase based on the thermophysical properties of the specimen, and avoids the use of a complex heat capacity which has no well-founded physical or thermodynamic meaning. Good agreement was found between experimental and predicted heat flow phase angles.

Keywords: TMDSC; Complex heat capacity; Phase lag; Heat transfer

1. Introduction

Thermal analysis is an invaluable research tool nowadays, as shown by the abundance of articles published every year in this area. Historical reviews usually reference Le Châtelier [1–3] as the first person to report temperature–time heating measurements at the turn of the 1880s. Fourteen years later, in 1904, Kurnakov [4] developed what is now known as the classical differential thermal analysis (DTA) set-up. It took nonetheless nearly half a century before DTA instruments became commercially available. Commercialization of DTA was shortly followed by the invention of differential scanning calorimetry (DSC). The principle of the DSC was first realized in a design described by Clarebrough et al. in 1952 [5]. DSC has virtually the identical field of application as DTA, but allows the quantification of heat flow. A little less than three decades later, Reading et al. [6–8] proposed to enhance DSC by imposing a sinusoidal temperature profile on top of the traditional heating ramp. This novel technique was designated as temperature modulated differential scanning calorimetry (TMDSC or MTDSC). It offers the possibility of deconvoluting the signal into an in-phase and an out-of-phase response, which allows for the distinction between reversible and irreversible heat flow [6,8,9]. Reading et al. [7] suggested also that the TMDSC response signals should be deconvoluted into c_p' and c_p'', the in-phase and out-of-phase component of a complex heat capacity. A complex product of heat capacity and thermal

*Corresponding author. Fax: +1-206-543-8386
E-mail address: jcseferis@aol.com (J.C. Seferis)

0040-6031/99/$ – see front matter
PII: S0040-6031(99)00112-4

conductivity had previously been reported by Birge and Nagel [10] in the case of ac-calorimetry. Numerous authors followed on the complex heat capacity path and the explanations are as numerous as the authors [8,11–18]. Aubuchon and Gill [8,11] attributed the existence of the imaginary part of the heat capacity, c_p'', to either kinetic events within the sample or to dissipation processes related to entropy production. Schawe [12,13] also associated c_p'' with dissipation and time-dependent thermal events. Later on Schawe refined his view of c_p'' by connecting it to changes in molecular mobility as well as entropy production in the system [14,15]. Jeong [16] drew analogies between c_p'' and dielectric susceptibility before concluding that c_p'' had an entropic origin and that it was representative of the entropy increase of the reservoir during one modulation cycle. Alig [17] proposed to compare sound absorption due to thermal relaxation in ultrasonic experiment with the complex heat capacity as measured in TMDSC. His conclusions were that c_p'' arises from the transfer of energy between the external and internal degrees of freedom. Höhne [18] offers yet another explanation which states that c_p'' should be related to the dissipated energy of the driving force of the time-dependent process. This plethora of interpretations leads to confusion and might have its origin in the misunderstanding of the phase lag observed in TMDSC. This phase lag has been mathematically explained by the existence of a complex heat capacity [11]. However, heat capacity is not a vector nor a tensor: it is a scalar. The heat capacity c_p is a material bulk property and it is therefore isotropic: heat capacity is the same in every direction. Moreover, c_p is a thermodynamic and not a kinetic property. If the heating of a body is not instantaneous it is not due to the value of its heat capacity; it is due to the fact that heat must diffuse into the material and this is governed by other thermophysical properties of the material – namely the thermal diffusivity α. Thermal diffusivity can be anisotropic since thermal conductivity k is anisotropic in some substances such as for instance carbon fibers. Thermal diffusivity can then be expressed as a tensor and, therefore, it is the material property responsible for the existence of a phase lag. Accordingly, a model of TMDSC should take into account α, along with the temperature gradients that it includes in its definition.

Most of the TMDSC models consider the sample temperature to be uniform throughout the specimen [6,8,12,19]. This completely ignores thermal diffusivity and the thermal gradients that it involves. Lacey et al. [20] attempted to include the thermal conductivity k in one of their models. Unfortunately, k was lumped into some calibration factor, and the geometry of the specimen was not taken into account and nor were the different temperature gradients. Melling et al. [21] modeled the temperature gradients in a DTA cell as early as 1969. However, only radial gradients were considered, and of course the boundary conditions did not include a sinusoidal modulation. Schenker and Stäger [22] proposed a model of heat transfer under TMDSC conditions, but in their case only axial diffusion was considered. Schawe and Winter [23] studied the influence of heat transfer from the heater to the specimen. They concluded that this heat transfer smeared the measured signal and that it was responsible for a decrease in heat flow amplitude and an increase in the heat flow phase. They did not however investigate the gradients within the specimen. It is only very lately that a detailed model of heat transfer was investigated, where both radial and axial temperature gradients were accounted for [24]. The analytical solution was calculated for a cylindrical shaped specimen considering top and side surfaces to follow the modulated temperature while the bottom surface was assumed insulated. It was found that the phase angle could be predicted by the introduction of two effective thermal diffusivities, Λ' and Λ'', and that c_p'' was an artifact due to simplistic mathematical representation of the problem [24]. The summation terms Λ' and Λ'' arise when solving the Sturm–Liouville problem associated with heat diffusion in a cylindrical geometry. Both Λ' and Λ'' are in units of m^2/s and can be regarded as the in-phase and out-of-phase effective thermal diffusivities, respectively [24].

The objective of this paper was to investigate further the model developed by Seferis et al. [24] and to compare it to experimental data. First, the time to reach the asymptotic (steady-state) temperature was estimated. Second, the temperature profiles within the specimen were calculated to assert the importance of temperature gradients. Finally, the heat flow phase lag obtained experimentally from different substances in the absence of transitions was compared to the model predictions.

2. Theory

A three-dimensional heat flow model of the TMDSC specimen shown in Fig. 1 was considered by Seferis et al. [24]. The temperature T was considered to be a function of the axial position z, the radial position r, and the time t. The heat transfer equation was expressed in cylindrical coordinates:

$$\frac{\partial T}{\partial t} = \alpha\left[\frac{1}{r}\frac{\partial}{\partial r}\left(r\frac{\partial T}{\partial r}\right) + \frac{\partial^2 T}{\partial z^2}\right], \tag{1}$$

where α is the thermal diffusivity of the specimen. Eq. (1) was solved with the following boundary conditions:

Specimen temperature equals to T_o initially :

$$T(r,z,0) = T_o, \tag{2}$$

Side surface temperature equals to that of the furnace T_b :

$$T(R,z,t) = T_b, \tag{3}$$

Top surface temperature equals to that of the furnace T_b :

$$T(r,0,t) = T_b, \tag{4}$$

No heat flux at the bottom surface :

$$-k\frac{\partial T}{\partial z}(r,L,t) = 0 \tag{5}$$

Symmetry condition at the center of the specimen :

$$\frac{\partial T}{\partial r}(0,z,t) = 0, \tag{6}$$

where the furnace (block) temperature is:

$$T_b = T_{bo} + bt + A\sin(\omega t). \tag{7}$$

In Eq. (7) b is the temperature ramp and A is the amplitude of the modulation. The pulsation ω is equal to 2π over the period of modulation. Solving analytically Eq. (1) along with Eqs. (2)–(7) yields [24]:

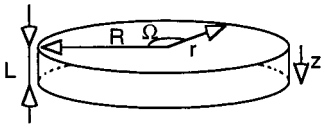

Fig. 1. The DSC pan considered to be a cylinder of radius R and length L. Cylindrical coordinates are used to solve the heat diffusion equation.

$$T(r,z,t) = \sum_{n=1}^{\infty}\left(\sum_{p=1}^{\infty}\left\{\frac{4}{\mu_p\lambda_n J_1(\lambda_n)}\right.\right.$$
$$\left[e^{-\frac{\kappa_{n,p}^2\alpha t}{R^2}}\left(T_o - T_{bo} + \frac{bR^2}{\alpha\kappa_{n,p}^2} + \frac{A\omega R^2\kappa_{n,p}^2}{\alpha\left(\kappa_{n,p}^4 + \frac{R^4\omega^2}{\alpha^2}\right)}\right)\right.$$
$$\left.-\frac{bR^2}{\alpha\kappa_{n,p}^2} - \frac{A\omega R^2}{\alpha\left(\kappa_{n,p}^4 + \frac{R^4\omega^2}{\alpha^2}\right)}\right.$$
$$\left.\left(\kappa_{n,p}^2\cos(\omega t) + \frac{\omega R^2}{\alpha}\sin(\omega t)\right)\right]J_o\left(\lambda_n\frac{r}{R}\right)$$
$$\left.\left.\cdot\sin\left(\mu_p\frac{z}{L}\right)\right\}\right) + T_b,$$

where λ_n, μ_p, and $K_{n,p}$ are eigenvalues. Although complex, the above expression provides a complete description of the temperature profile in a typical TMDSC experiment. The first term inside the square bracket of Eq. (8) accounts for the transient behavior and vanishes at sufficiently long times (exponential decay). The second term in the square bracket (containing b) accounts for the effect of the heating ramp on the temperature profile, while the third term in these brackets accounts for the temperature amplitude. The terms located on the right-hand side of the square bracket of Eq. (8) are position terms and allow the determination of the temperature profiles along the radial and axial directions of the specimen.

In TMDSC the specimen temperature is typically recorded by thermocouples located under the pan, which means that the temperature reading is that of the r=0 and z=L position, L being the height of the specimen. At sufficiently large times, the temperature difference between the reference and the sample specimens can be expressed as [24]:

$$T_r - T_s = bR^2\left(\frac{1}{\alpha_r} - \frac{1}{\alpha_s}\right)\sigma$$
$$+ A\omega R^2\sqrt{\left(\frac{1}{\Lambda_r'} - \frac{1}{\Lambda_s'}\right)^2 + \left(\frac{1}{\Lambda_r''} - \frac{1}{\Lambda_s''}\right)^2}$$
$$\sin(\omega t + \psi), \tag{9}$$

with

$$\tan\psi = \frac{1/\Lambda_r'' - 1/\Lambda_s''}{1/\Lambda_r' - 1/\Lambda_s'}, \tag{10}$$

where A is the modulation amplitude, R the specimen radius, T the temperature, b the linear heating rate, Λ' and Λ'' the effective thermal diffusivities, α the thermal diffusivity, σ a summation term, ψ the phase angle between the block temperature and the temperature difference between sample and reference, and ω the pulsation of the modulation. Indices r and s refer to reference and sample, respectively. A more detailed description of the different terms can be found in [24].

Eq. (9) can be rewritten under the form:

$$\Delta T = T_r - T_s = \overline{\Delta}T + \tilde{\Delta}T = \overline{\Delta}T + |\tilde{\Delta}T| \sin(\omega t + \psi), \quad (11)$$

where $\overline{\Delta}T$ is the underlying part of the temperature difference between the reference and the sample, $\tilde{\Delta}T$ is the cyclic part of this temperature difference, and $|\tilde{\Delta}T|$ is the amplitude of the cyclic part.

In many TMDSC papers, the angle reported is the heat flow phase, which is defined as the angle between the heat flow and the derivative of the temperature [8,11]. This angle will be denoted by γ in this paper. The heat flow Q is given by [8]:

$$\frac{dQ}{dt} = \frac{\Delta T}{R_{th}}, \quad (12)$$

where R_{th} is a thermal resistance. Solving Eq. (12), Eq. (11) yields:

$$Q = \frac{1}{R_{th}}\left[\overline{\Delta}T \cdot t + \frac{1}{\omega}|\tilde{\Delta}T|\{-\cos(\omega t + \Psi)\}\right] = \frac{1}{R_{th}}\left[\overline{\Delta}T \cdot t + \frac{1}{\omega}|\tilde{\Delta}T| \sin\left(\omega t + \Psi - \frac{\pi}{2}\right)\right]. \quad (13)$$

The derivative of the modulated temperature is:

$$\frac{dT}{dt} = \frac{d}{dt}[T_{bo} + b \cdot t + A \sin(\omega t)] = b + A\omega \cos(\omega t) = b + A\omega \sin\left(\omega t + \frac{\pi}{2}\right) \quad (14)$$

It follows from Eqs. (13) and (14) that γ and ψ are supplementary angles:

$$\gamma = \pi - \psi. \quad (15)$$

Eq. (15) is valid only in the absence of thermal events and instrumental phase. Every instrument contributes to the phase lag by its inherent thermophysical and thermodynamical properties (furnace thermal resistance, non-adiabaticity, etc). This will modify Eq. (15) by the addition of an extra contribution:

$$\gamma = \pi - \psi - \gamma_{instr}. \quad (16)$$

This instrumental phase lag γ_{instr} can be determined by a calibration run [23]. This instrumental lag will depend on the experimental temperature range, ramp rate, and other experimental parameters. Eqs. (10) and (16) allow the calculation of the heat phase γ with the knowledge of the effective thermal diffusivities Λ' and Λ. These are computed from the material thermophysical properties [24]. Therefore, γ is expected to be depending upon the nature of the sample material.

3. Experimental

Three polymeric compounds were obtained from Aldrich. Poly (ethylene terephthalate) (PET) was provided under the form of pellets which were crushed after immersion in liquid nitrogen. Poly (vinyl chloride) (PVC) and poly (methyl methacrylate) (PMMA) were secondary standards and were used as received. A sapphire sample was supplied by TA Instruments and was used as received in its original aluminum pan. Finally, a fiberglass sample was prepared from a style 1581 fabric manufactured by Clark and Schwebel.

TMDSC experiments were conducted on a DSC 2910 from TA Instruments equipped with a liquid nitrogen cooling accessory (LNCA). Heating rate was set to 1°C/min, with a 0.5°C modulation every 60 s. Temperature within the cell was equilibrated at −25°C prior to the experimental run. All runs were terminated once a temperature of 100°C was reached. The phase angle between the derivative of the modulated temperature and the modulated heat flow were measured when the temperature was approximately 20°C.

4. Results and discussion

Numerical simulations of the specimen temperature evolution and profiles were carried out for a PET sample and an aluminium pan reference using the parameters of Table 1 with a procedure described previously [24]. The modulation amplitude was set

Table 1
Parameters used for the numerical simulation

Parameter	Symbol	Value	Unit
Modulation amplitude	A	0.5	K
Radius of the specimen	R	0.0033	m
Height of specimen	L	0.00074	m
Initial temperature of the sample	T_0	293	K
Isothermal experiment	b	0	K/s
Aluminium pan	α_r	9.71×10^{-5}	m^2/s
Modulation period of 60 s	ω	$2\pi/60$	rad/s

Table 2
True and effective thermal diffusivities of substance of interest [25–27]

	α (m^2/s)	Λ'	Λ''
PET	0.093×10^{-6}	1.5479×10^{-5}	3.6319×10^{-6}
PMMA	0.113×10^{-6}	2.2451×10^{-5}	4.3369×10^{-6}
PVC	0.346×10^{-6}	2.0351×10^{-4}	1.2843×10^{-5}
Glass fiber	0.431×10^{-6}	3.1533×10^{-4}	1.5975×10^{-5}
Sapphire	8.300×10^{-6}	3.1533×10^{-4}	3.0684×10^{-4}
Aluminum	97.14×10^{-6}	15.9740	0.0036

to 0.5 K every 60 s at the quasi-isothermal temperature T_0 of 293 K. Fig. 2 shows the temperature evolution at the center bottom of the specimens over one period of modulation. The transient terms, which were previously discarded [24], are now accounted for. The transient terms were found to be insignificant for the aluminum reference. They did, however, have an influence on the temperature evolution at very early times for the PET sample as shown by the comparison of curves 2 and 3 in Fig. 2. After about 1/8 of a period, curves 2 and 3 merged together and were indistinguishable as the temperature of PET reached its asymptotic behavior. The aluminium reference, on the other hand, reached its asymptotic behavior almost immediately. No distinction was possible between the temperature computed with and without the transient terms; this is why only one curve was displayed for the reference. This behavior was a result of the high thermal diffusivity of aluminum which was three orders of magnitude above that of PET, as shown in Table 2. Since both reference and sample reached their asymptotic behavior quickly, the following numerical simulations of the temperature profiles within the specimens were carried out without the transient terms, assuming that the observations were made after one full period (t=60 s). The temperature profiles within the specimens are displayed in Figs. 3 and 4. Both sample and reference displayed identical

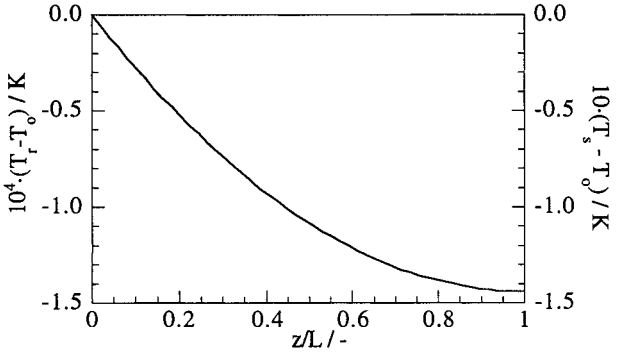

Fig. 3. Temperature profile along the axial direction of a PET sample at t=60 s.

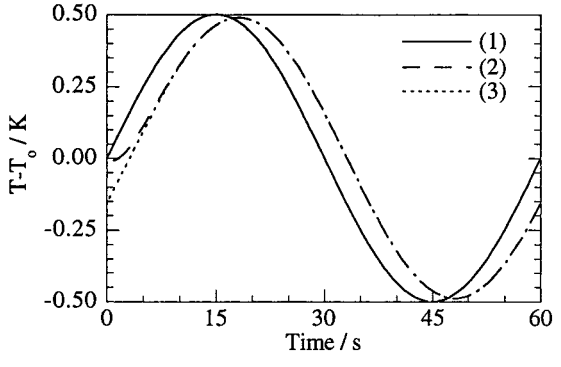

Fig. 2. Transient evolution of (1) aluminium reference (2) PET sample (3) PET sample without the transient terms.

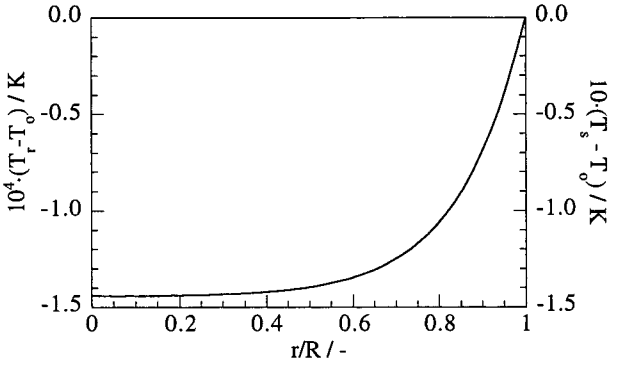

Fig. 4. Temperature profile along the radial direction of a PET sample at t=60 s.

temperature profiles, only with scale differences. All the curves were calculated from Eq. (8) without transient terms; it is therefore not surprising that the curve shape was identical when a closer look at Eq. (8) is taken. The third term inside the square brackets of Eq. (8), which depends only on the experimental conditions and on the specimen thermophysical properties, sets the scale of the profile, while the last terms of the equation set the axial and radial dependence. Hence the temperature profiles shown in Figs. 3 and 4 apply for any type of specimen, only the scale will change depending upon the sample material. In Figs. 3 and 4, the left-hand side scale corresponds to the aluminum reference, while the right-hand side scale corresponds to the PET sample. In Fig. 3, it is seen that the temperature of the reference (T_r) varied by approximately 1.5×10^{-4} K between the center top ($z=0$) and center bottom ($z=L$) of the pan while the PET sample temperature (T_s) experienced a change three orders of magnitude greater, i.e. the temperature difference in the sample between top and bottom was 0.15 K. The axial temperature profile flattens out at $z=L$, which was required by the boundary condition of Eq. (5). The temperature at the top surface ($z=0$) is set to T_b by the boundary condition of Eq. (4) and T_b turns out to be equal to T_0 after one period of modulation in the case of a quasi-isothermal experiment, hence the zero value of $T-T_0$ at this particular point. The reference and sample temperature profiles along the radial direction, Fig. 4, showed temperature differences of the same magnitude as in the axial direction. In Fig. 4, the radial temperature profile flattens out as the radial variable r goes to zero to satisfy Eq. (6). Eq. (3) is satisfied by having $T-T_0=0$ at $r=R$. From Figs. 3 and 4, it is shown that temperature differences of about one and a half tenths of a Kelvin can exist within a sample such as PET. These gradients are due to the relatively low thermal diffusivity of the specimens and should be taken into account when deconvoluting the TMDSC signals to avoid the use of a complex heat capacity of doubtful physical origin.

The mathematical model was also tested against experimental data. Phase lag calculations were investigated for five different materials of various thermal diffusivity and were compared to heat flow phase as measured experimentally. A typical TMDSC thermogram is shown in Fig. 5. The modulated heat flow and the derivative of the modulated temperature differed

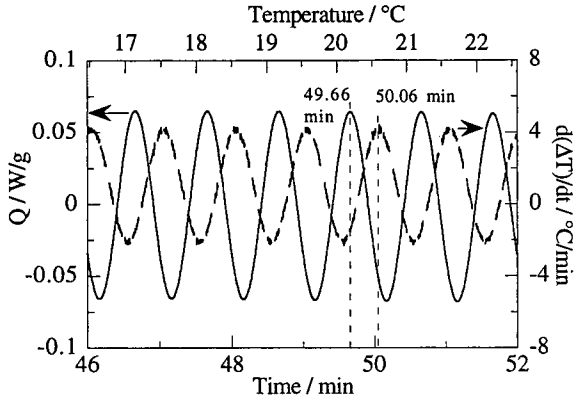

Fig. 5. Example of TMDSC thermo-analytical curve for the determination of the heat flow phase lag. Sample shown in PET.

by 0.4 min, which corresponds to a phase lag of 144°. The model predicted a phase lag of 103° for PET. The difference between these two values is explained by the instrumental contribution to phase lag, which turned out to be about 41°. The phase lag calculation and measurements are summarized in Table 3 for all five compounds studied. The calculated heat flow phase decreased with increasing thermal diffusivity, as expected since the greater the thermal diffusivity, the faster the heat transfer, hence smaller phase lag. The experimental data paralleled that trend, except for the PVC sample. This might be due to the use of a literature value of thermal diffusivity that did not correspond to that of our specific PVC sample. The differences between the experimental and calculated values were explained by the instrument contribution to the phase lag, which was neglected in the mathematical model. The instrument phase lag, displayed in the third column of Table 3, was found to be constant with a value of about 40°. Only the PVC showed an instrumental phase lag different from 40°, and this was probably because of the reasons mentioned earlier: the

Table 3
Calculated and experimental heat flow phase of the five selected materials ordered by increasing thermal diffusivity

	γ_{calc}/°	γ_{exp}/°	$\gamma_{exp}-\gamma_{calc}$/°
PET	103.2	144.0	40.8
PMMA	101.0	140.4	39.4
PVC	93.6	147.6	54.0
Glass fiber	92.6	133.2	40.6
Sapphire	90.2	122.4	32.2

calculated value of PVC must have been underestimated by our model, which leads to a higher instrumental phase lag. The instrumental phase lag is expected to be constant for identical TMDSC operating conditions and parameters, and this is what is generally shown in Table 3.

5. Conclusions

An elaborate model of heat transfer in a TMDSC sample was evaluated. The model was used to determine the importance of the transient terms of the temperature evolution at early times. It was found that the asymptotic temperature was reached after one eighth of a period of modulation already in the case of a PET sample. Simulation of the temperature distribution within the same sample revealed that difference of as much as a third of the temperature amplitude can exist along the radial and axial dimensions. These temperature gradients are not accounted for in traditional TMDSC model and lead to the use of a complex heat capacity of dubious physical or thermodynamical basis. The investigated model accounted for thermal diffusivity and was able to predict the heat flow phase based on an effective thermal diffusivity rather than a complex heat capacity. Experimental data confirmed the model predictions and a $\sim 40^{\circ}$ phase lag contribution from the instrument was found.

Acknowledgements

The authors express their appreciation to T.A. Instruments for continuous support to the Polymeric Composites Laboratory at the University of Washington. Support for this work was also provided by The Boeing Company through the Boeing–Steiner Professorship.

References

[1] H. Le Châtelier, Comptes Rendus Hebdomadaires des Séances de l'Académie des Sciences 104 (1887) 1443.
[2] B. Wunderlich, Thermal Analysis, Academic Press, San Diego, 1990.
[3] M.I. Pope, M.D. Judd, Differential Thermal Analysis: a Guide to the Technique and its Application, Heyden, London, 1977.
[4] N.S. Kurnakov, Zeitschrift für anorganische Chemie 42 (1904) 184.
[5] L.M. Clarebrough, M.E. Hargreaves, D. Michell, G.W. West, Proc. Roy. Soc., Ser. A: Math. Phys. Sci. 215 (1952) 507.
[6] M. Reading, E. Elliott, V.L. Hill, J. Thermal Anal. 40 (1993) 949.
[7] M. Reading, R. Wilson, H.M. Pollock, Proceedings of the 23rd Conference of the NATAS, Jacksonville, FL, 1994, p. 2.
[8] P.S. Gill, W.R. Sauerbrunn, M. Reading, J. Thermal Anal. 40 (1993) 931.
[9] J.C. Seferis, I.M. Salin, P.S. Gill, M. Reading, Proc. Natl. Acad., Athens 67 (1992) 311.
[10] N.O. Birge, S.R. Nagel, Phys. Rev. Lett. 54 (1985) 2674.
[11] S.R. Aubuchon, P.S. Gill, J. Thermal Anal. 49 (1997) 1039.
[12] J.E.K. Schawe, Thermochim. Acta 260 (1995) 1.
[13] J.E.K. Schawe, Thermochim. Acta 271 (1996) 127.
[14] J.E.K. Schawe, G.W.H. Höhne, Thermochim. Acta 287 (1996) 213.
[15] J.E.K. Schawe, G.W.H. Höhne, J. Thermal Anal. 46 (1996) 893.
[16] Y.-H. Jeong, Thermochim. Acta 304 305 (1997) 67.
[17] I. Alig, Thermochimica Acta 304 305 (1997) 35.
[18] G.W.H. Höhne, Thermochim. Acta 304 305 (1997) 121.
[19] A. Boller, Y. Jin, B. Wunderlich, J. Thermal Anal. 42 (1994) 307.
[20] A.A. Lacey, C. Nikopoulos, M. Reading, J. Thermal Anal. 50 (1997) 279.
[21] R. Melling, F.W. Wilburn, R.M. McIntosh, Anal. Chem. 41 (1969) 1275.
[22] B. Schenker, F. Stäger, Thermochim. Acta 304 305 (1997) 219.
[23] J.E.K. Schawe, W. Sinter, Thermochim. Acta 298 (1997) 9.
[24] F.U. Buehler, C.J. Martin, J.C. Seferis, J. Thermal Anal. 54 (1998) 501.
[25] F.P. Incropera, D.P. De Witt, Fundamentals of Heat and Mass Transfer, Wiley, New York, 1990.
[26] J. Brandrup, E.H. Immergut, Polymer Handbook, Wiley, New York, 1989.
[27] Y.S. Touloukian, R.W. Powell, C.Y. Ho, M.C. Nicolaou, in: Y.S. Touloukian (Ed.), Thermophysical Properties of Matter, vol. 10, IFI/Plenum Press, New York, 1973.